PROCEEDINGS OF SCIENCE

Measurement of sparse vs. dense atmospheric secondary particles from cosmic ray showers using coincident signals on various counters in a neutron monitor

Kullapha Chaiwongkhot,[a,*] **David Ruffolo,**[a] **Alejandro Sáiz,**[a] **Warit Mitthumsiri,**[a] **Poompong Chaiwongkhot,**[b] **Chanoknan Banglieng,**[c] **Pierre-Simon Mangeard,**[d] **Paul Evenson**[d] **and Jidapa Lakronwat**[e]

[a] *Department of Physics, Faculty of Science, Mahidol University, Bangkok 10400, Thailand*
[b] *National Astronomical Research Institute of Thailand (NARIT), Chiang Mai, Thailand*
[c] *Division of Physics, Faculty of Science and Technology, Rajamangala University of Technology Thanyaburi, Pathum Thani, Thailand*
[d] *Bartol Research Institute, Department of Physics and Astronomy, University of Delaware, Newark, DE, USA*
[e] *Department of Physics, Faculty of Science, Kasetsart University, Bangkok, Thailand*

E-mail: kullapha.cha@mahidol.ac.th, david.ruf@mahidol.ac.th

For the Princess Sirindhorn Neutron Monitor in Thailand, we find that the cross-counter leader fraction (XLF), i.e., inverse of multiplicity across counters, depends on counter separation and differs for end and middle counter tubes. Multiplicity at small separation can be attributed to single secondary particles, while multiplicity at large separation indicates multiple secondaries from the same cosmic ray shower. The end/middle differences are clarified using follow-up measurements of 1) analog neutron signals from selected counters and 2) digital timing data from all counters for events of interest. Considering Counters 17 and 18 at the edge of the monitor, triggering on either counter leads to the same event rate on the other, so small-separation XLF depends on the count rate of the first (triggering) counter, which is lower for an end counter. To examine large-separation multiplicity, due to multiple secondaries, an FPGA-based readout system was triggered by Counter 2 followed by Counter 18 within 250 microseconds, while also monitoring Counter 10 in between. Counter 10 exhibited an enhanced rate, indicating a few events that densely "carpeted" the neutron monitor, but the majority of triggers involved a sparse distribution of isolated secondary particles. This is consistent with the digital timing data from all counters and end/middle differences in XLF.

38th International Cosmic Ray Conference (ICRC2023)
26 July - 3 August, 2023
Nagoya, Japan

[*] Speaker

1. Introduction

Cosmic ray particles can be detected either directly in space, or indirectly by means of air showers generated by their interactions in Earth's atmosphere, called secondary cosmic rays. The Earth's magnetic field serves as a spectrometer, only allowing particles above a local cutoff (threshold) rigidity to reach the atmosphere. Neutron monitors (NMs) are standard ground-based instruments for measurement of secondaries' time variations. Therefore NM stations have been established worldwide, and each provides information about cosmic rays at rigidity above its local cutoff.

In a neutron monitor, atmospheric secondary particles from cosmic ray showers interact in lead to produce low-energy tertiary neutrons that are detected in a proportional counter. Studying the timing along the complicated path of a neutron inside the neutron monitor [1] is important for Monte Carlo simulations and studying the tertiary neutron multiplicity for which the inverse is referred to here as the "leader fraction" [2].

In this work, for a given pair of neutron counters, we adapt experimental techniques to study the cross-counter leader fraction (XLF) which is defined as the fraction of tertiary neutron counts in the second counter which is not temporally associated with counts in the first counter. The value of XLF relates to the efficiency of each counter in a given pair, depending on each counter's location. Having less nearby lead producer, an end counter provides a lower count rate, while the middle counters have higher chances to detect neutrons from secondary cosmic ray interactions due to having more nearby lead.

Over a certain duration, the average values of XLF for a given pair of counters can be calculated from time-delay histograms as described in more detail in [3]. Recent measurements of XLF for different pairs of counters as a function of counter separation and location [4], have found that:

- Tertiary neutrons from the same atmospheric secondary particles interacting with the lead producer dominate associated counts among neighboring counters, resulting in the XLF that depends on whether the *first* counter is an end or a middle counter (specifically, XLF is lower if the first counter is the end counter), and
- Associated counts detected in distant counters are produced by multiple atmospheric secondary particles from the same primary cosmic ray, resulting in the XLF that depends on whether the *second* counter is an end or middle counter (specifically, XLF is higher if the second counter is an end counter).

Here we study measurements of neutron signals from linear amplified outputs at the Princess Sirindhorn Neutron Monitor (PSNM), an 18-counter NM64 detector [5] at 2560 m altitude at Doi Inthanon, Thailand (18.59°N, 98.49°E) using a 4-channel oscilloscope, in order to further investigate these phenomena.

2. Experiment Setup

The experiment was setup in two configurations including the time delay distribution measurements of multiple counts from the secondary events in a pair of neighboring counters and the measurement of the coincident counts between distant counters.

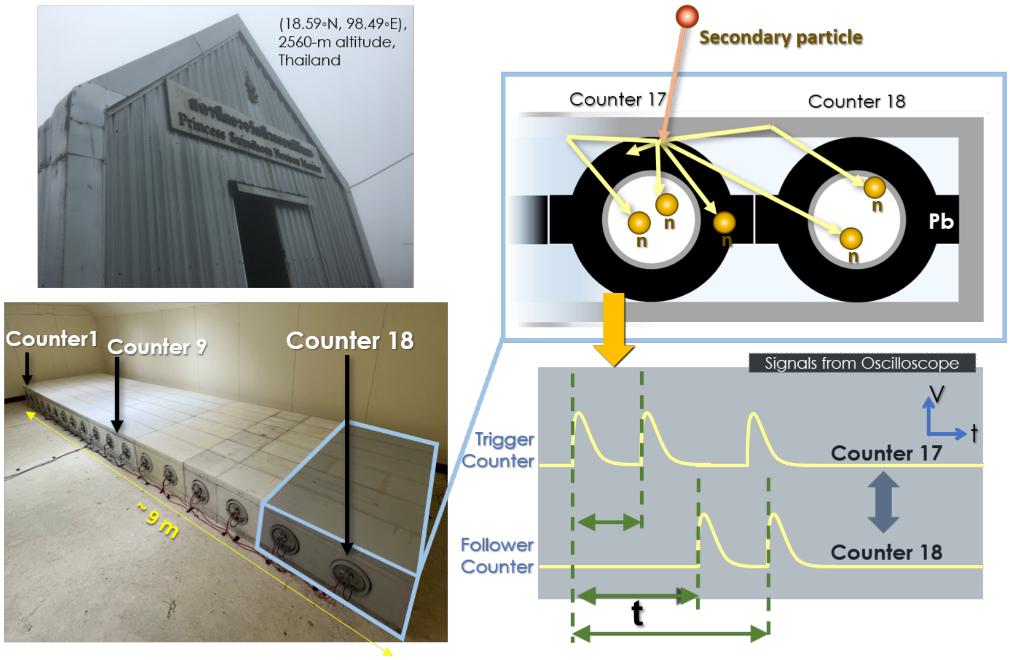

Figure 1: The experiment setup for the measurement of multiple counts from secondary events in a pair of neighboring counters. Counter number 17 and 18 were used to provide the trigger pulse signal for other counters. The pulses from the triggered and neighboring counters were collected by an oscilloscope within 6 ms time window.

To study multiple counts from the secondary events in a pair of neighboring counters, an oscilloscope (DS1104Z Plus, Rigol, China) was set to acquire the linear pulse signal of counters 17 and 18. For this measurement, we set the trigger of the oscilloscope to counter 17 and collected the data from counters 2, 11, 17, and 18. The trigger was set to either counter 17 and 18, and collected the pulses from the others. By using of 30,000 sampling points, the shape of the signal pulse were collected within a 6-ms time window for each channel of the oscilloscope. Figure 1 shows the photo of the PSNM and the 18 NM64 counters inside the building. Counter 17 and 18 is located on the edge of the counters array. The time delay(t) between the signal pulses from the trigger pulse was done in the post-analysis.

An FPGA-based readout system was developed for more efficient collection of neutron events on two distant counters (Counters 2 and 18). The criteria of a time coincident was programmed on an FPGA Trainer Board (Nexys A7-50T; Digilent, Inc.) to generate a coincident pulse (TTL) if there is a neutron signal pulse detected from Counter 2 and followed by at least one neutron signal pulse detected from counter 18 within a 250-microsecond time window. The 4-channels oscilloscope was set to save the linear pulse from counter2, 10, and 18 in 6-ms time window when the coincident pulse was detected. The measurement was performed from 2021 December 26 at 5:26 UT to December 28 at 02:59 UT at the PSNM station.

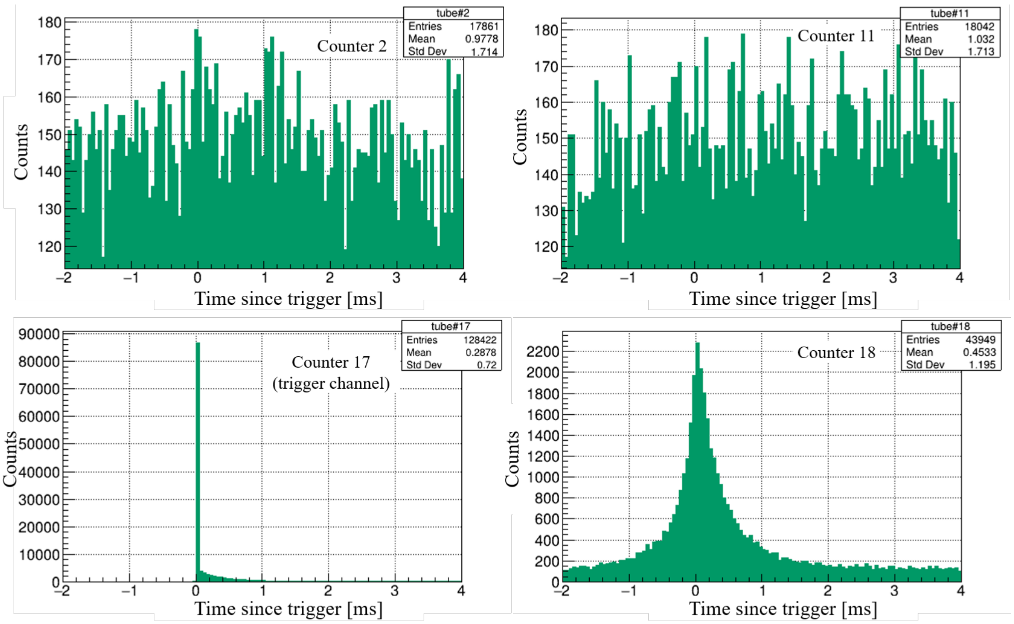

Figure 2: Distribution in time t (relative to a trigger from counter 17) of pulses with $-2.0 \leq t < 4.0$ ms for PSNM counters 2, 11, 17 (trigger) and 18.

3. Preliminary Results and Discussions

3.1 Multiple counts from the secondary events in a pair of neighboring counters

This measurement was performed from 2021 July 27 at 05:48 UT to July 28 at 05:18 UT and from July 28 at 09:51 UT to July 29 at 03:16 UT, 2021, and in total 83,000 triggered events were collected. Figure 2 shows the time distribution of all pulses related to the trigger pulses from counter 17 within the 6 ms time window of the oscilloscope. In addition, with the same setup and changing the trigger to counter 18, data were collected from July 29 at 09:50 UT to July 30 at 03:34 UT and from July 30 at 03:48 UT to 05:13 UT. The time distribution from the 38,803 triggered events of this configuration is shown in Figure 3. The time distribution coincident with the trigger time of the neighboring counter far above the background level of the chance coincident events is obvious for the both configurations.

Figure 4 indicates the roughly equal event rate distributions of the counter next to the trigger counter from the both configurations of the measurement. The average multiplicity of the neighboring counter after subtracting the background level was found to be different at 1.387 or 1.412 for the triggering at counter 17 or 18, respectively. These results have implications for recent measurements of time delays between neutron events in different counters by our group [3, 4], confirming that the difference in leader fraction (inverse multiplicity) mostly relates to the base count rate of the first counter and is therefore lower if that is an end counter.

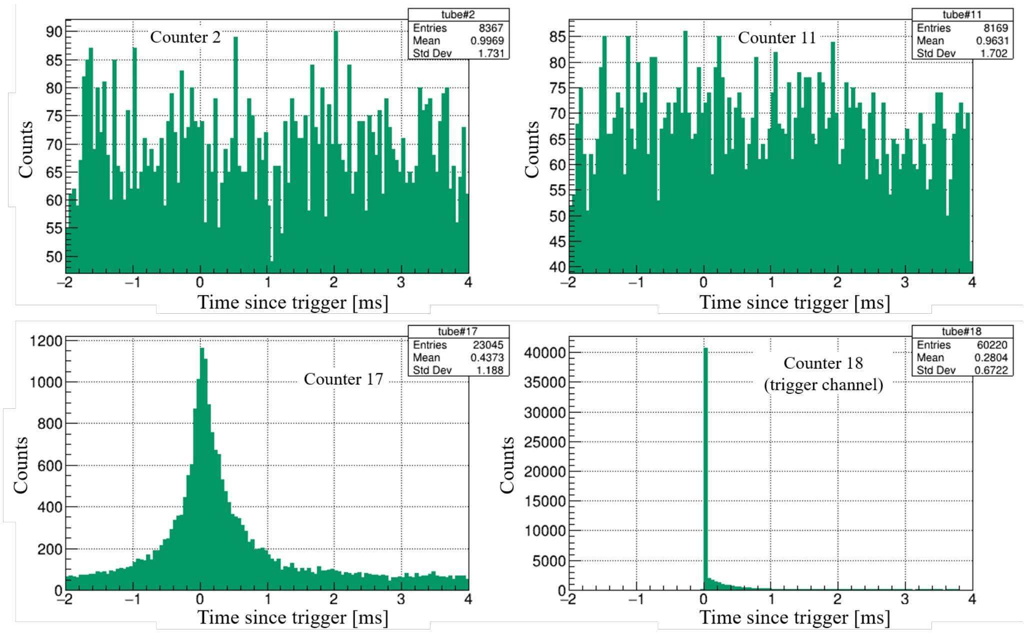

Figure 3: Distribution in time t (relative to a trigger from counter 18) of pulses with – 2.0 ≤ t < 4.0 ms for PSNM counter 2, 11, 17 and 18(trigger).

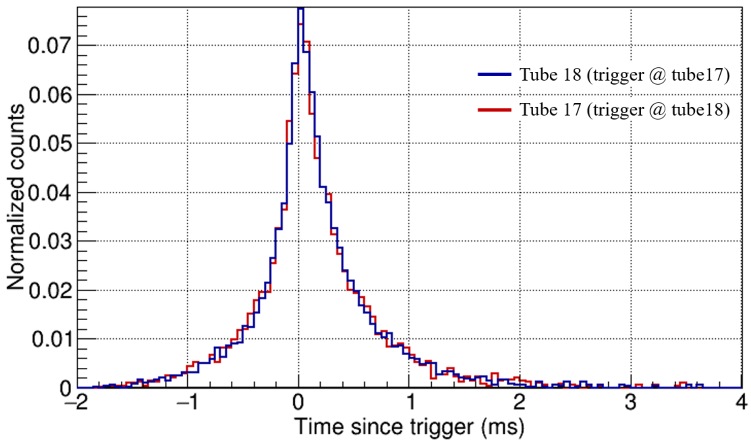

Figure 4: Time distribution of the count rate per bin [Hz] of the neighbor counters of the trigger counters; counter 18 where triggering at counter 17 (blue) and counter 17 where triggering at counter 18 (red).

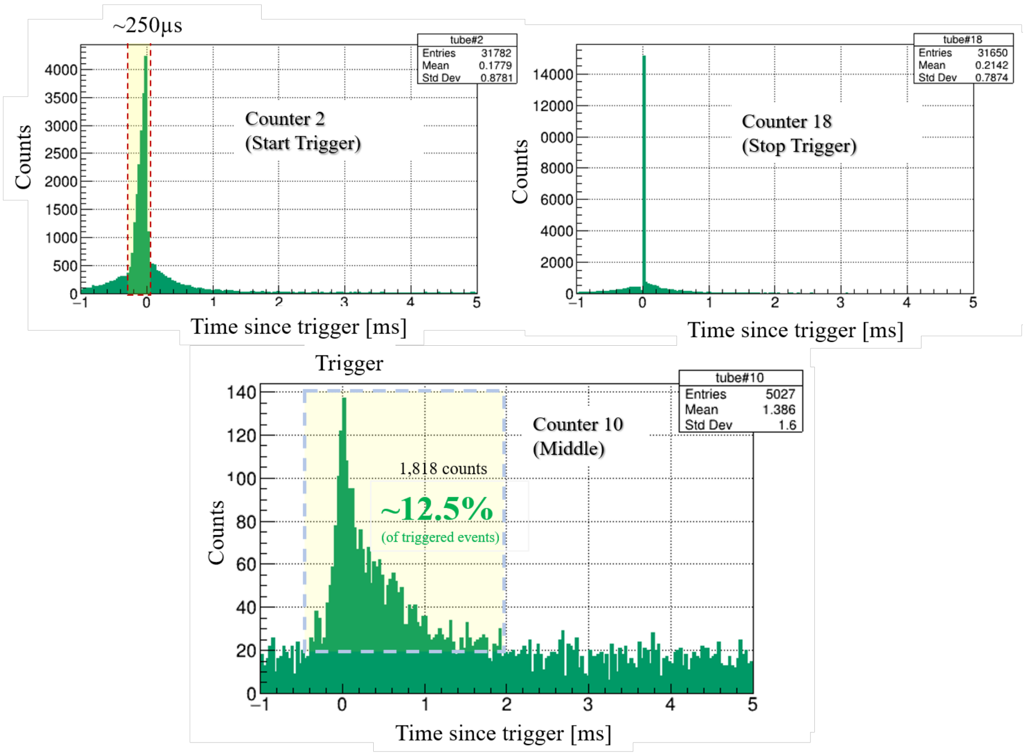

Figure 5: Distribution in time (relative to a coincident pulse trigger) of pulses with $-1.0 \leq t < 5.0$ ms for PSNM.

3.2 Coincident counts between distant counters

The measurement was performed from 2021 December 26 at 5:26 UT to December 28 at 02:59 UT at the PSNM station. Figure 5 indicated the time distributions from counter 2 (top left), 18 (top right) and 10 (bottom). The time distribution of counter 2 shows the peak within 250 us corresponding to the coincident criteria that the first pulse has to come from counter 2. The time distribution of counter 18 presents the spike at 0 us which is the same time as when the coincident trigger signals were generated by the FPGA. The time distribution of counter 10 indicates a small fraction of the cosmic ray events that triggered both counters 2 and 18 also led to neutron events on counter 10. This indicates a few air-shower events that densely “carpeted” the neutron monitor, at only around 12.5% of the triggered events. Thus, the majority of the coincidences apparently involved a sparse distribution of isolated secondary particles near counter 2 and near counter 18 and not near the intermediate counter 10. These results are consistent with a cross-counter leader fraction dependence on the count rate of the second counter, which should be higher if the second counter is the end counter due to the lower efficiency of the less lead producer nearby the counter.

The data acquisition of the neutron monitor was upgraded to collect the data with the same coincident criteria as the oscilloscope measurement which of 250 us time window started from a pulse of counter number 2 and counter number 18 of all counters at PSNM. The plot Figure 6(left) is a histogram of all coincident events for each number of counters that detected a signal from 1 ms before the coincident trigger signal until 2 ms after it. The distribution has the main peak at 2

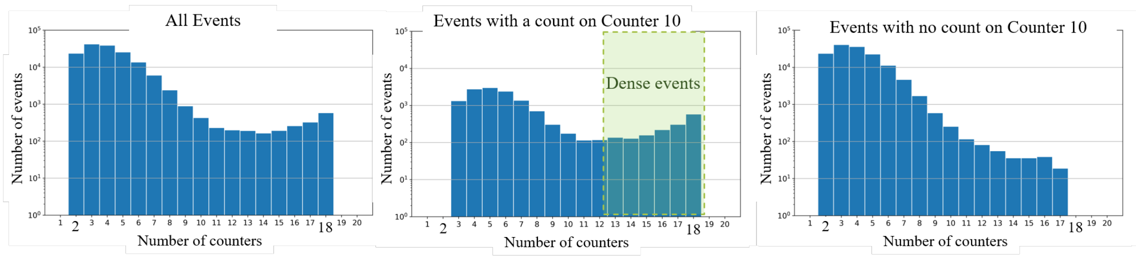

Figure 6: Coincident events for each number of counters collected from the upgraded NM DAQ.

counters. The events with a count on counter 10 on the middle histogram in Figure 6 indicates the lower number of events compare with the histogram of the events with no count on counter number 10 in Figure 6 (right). This result confirmed that most coincident events have sparse multiple secondaries. This is consistent with a cross-counter leader fraction dependence on the count rate of the second counter, which should be higher if the second counter is the end counter due to the lower efficiency because of the less nearby the counter. A distribution of some dense secondary events was also found from the large number of triggered counters in this measurement.

4. Acknowledgements

This research has been supported by Thailand Science Research and Innovation (RTA6280002), by the National Science and Technology Development Agency (NSTDA) and National Research Council of Thailand (NRCT): High-Potential Research Team Grant Program (N42A650868), and from the NSRF via the Program Management Unit for Human Resources & Institutional Development, Research and Innovation (B37G660015). Support was also provided to K.C. from postdoctoral research sponsorship of Mahidol University and J.L. from the Development and Promotion of Science and Technology Talents Project (DPST).

References

[1] K. Chaiwongkhot, D. Ruffolo, W. Yamwong, J. Prabket, P.S. Mangeard, A. Sáiz et al., *Measurement and simulation of the neutron propagation time distribution inside a neutron monitor*, *Astroparticle Physics* **132** (2021) 102617.

[2] D. Ruffolo, A. Sáiz, P.S. Mangeard, N. Kamyan, P. Muangha, T. Nutaro et al., *Monitoring Short-term Cosmic-ray Spectral Variations Using Neutron Monitor Time-delay Measurements*, *Astrophys. J.* **817** (2016) 38.

[3] A. Sáiz, W. Mitthumsiri, D. Ruffolo, P. Evenson and T. Nutaro, *Measurement of cross-counter leader fractions in an 18NM64: Detecting single and multiple atmospheric secondaries*, in *35th International Cosmic Ray Conference (ICRC2017)*, vol. 301 of *International Cosmic Ray Conference*, p. 47, July, 2017, DOI.

[4] A. Sáiz, W. Mitthumsiri, D. Ruffolo, P. Evenson and T. Nutaro, *Detecting Single and Multiple Atmospheric Secondaries in an 18NM64*, in *36th International Cosmic Ray Conference (ICRC2019)*, vol. 36 of *International Cosmic Ray Conference*, p. 1145, July, 2019, DOI.

[5] C.J. Hatton and H. Carmichael, *Experimental Investigation of the NM-64 Neutron Monitor*, *Canadian Journal of Physics* **42** (1964) 2443.